Tug-of-war between driver and passenger mutations in cancer and other adaptive processes

Christopher D. McFarland[a], Leonid A. Mirny[a,b,c,1], and Kirill S. Korolev[b,d,1]

[a]Graduate Program in Biophysics, Harvard University, Boston, MA 02115; [b]Department of Physics and [c]Institute for Medical Engineering and Science, Massachusetts Institute of Technology, Cambridge, MA 02139; and [d]Department of Physics and Program in Bioinformatics, Boston University, Boston, MA 02215

Edited* by Herbert Levine, Rice University, Houston, TX, and approved August 7, 2014 (received for review March 7, 2014)

Cancer progression is an example of a rapid adaptive process where evolving new traits is essential for survival and requires a high mutation rate. Precancerous cells acquire a few key mutations that drive rapid population growth and carcinogenesis. Cancer genomics demonstrates that these few driver mutations occur alongside thousands of random passenger mutations—a natural consequence of cancer's elevated mutation rate. Some passengers are deleterious to cancer cells, yet have been largely ignored in cancer research. In population genetics, however, the accumulation of mildly deleterious mutations has been shown to cause population meltdown. Here we develop a stochastic population model where beneficial drivers engage in a tug-of-war with frequent mildly deleterious passengers. These passengers present a barrier to cancer progression describable by a critical population size, below which most lesions fail to progress, and a critical mutation rate, above which cancers melt down. We find support for this model in cancer age–incidence and cancer genomics data that also allow us to estimate the fitness advantage of drivers and fitness costs of passengers. We identify two regimes of adaptive evolutionary dynamics and use these regimes to understand successes and failures of different treatment strategies. A tumor's load of deleterious passengers can explain previously paradoxical treatment outcomes and suggest that it could potentially serve as a biomarker of response to mutagenic therapies. The collective deleterious effect of passengers is currently an unexploited therapeutic target. We discuss how their effects might be exacerbated by current and future therapies.

evolution | mathematical modeling | simulations | cancer genomics | chemotherapy

Although many populations evolve new traits via a gradual accumulation of changes, some adapt very rapidly. Examples include viral adaptation during infection (1), the emergence of antibiotic resistance (2), artificial selection in biotechnology (3), and cancer (4). Rapid adaptation is characterized by three key features: (*i*) the availability of strongly advantageous traits accessible by rare mutations, (*ii*) an elevated mutation rate (1), and (*iii*) a dynamic population size (5). Because traditional theories of gradual adaptation are not applicable under these conditions, new approaches are needed.

Cancer progression is an example of a rapidly adapting population: cancers develop as many as 10 new traits (6), exhibit a high mutation rate (6–8), and rapidly change in population size (9). Progression is driven by a handful of mutations (10) and chromosomal abnormalities (11) in cancer-related genes (oncogenes and tumor suppressors), collectively called "drivers." Drivers are beneficial to cancer cells as they facilitate uncontrolled proliferation and other hallmarks of cancer (6). Drivers, however, arise alongside thousands of other mutations/alterations, called "passengers," that are randomly dispersed throughout the genome, are nonrecurrent in patients, and have no immediate beneficial effect (10).

Passengers have previously been assumed to be neutral and largely ignored in cancer research, yet growing evidence suggests that they can be deleterious to cancer cells and play an important role in both cancer progression and clinical outcomes. Previously, we showed that deleterious passengers readily accumulate during tumor progression and exhibit signatures of damaging mutations (12). Passenger mutations and chromosomal abnormalities, including aneuploidy, can be deleterious via a variety of mechanisms such as direct loss-of-function (13), cytotoxicity from protein disbalance and aggregation (14), or by eliciting an immune response (15).

Although the role of deleterious mutations in cancer is largely unknown, their effects on natural populations have been extensively studied in genetics (16–18). The accumulation of deleterious mutations can cause population extinction by Muller's ratchet and mutational meltdown (16, 19). How this applies to rapidly adapting populations with a varying size and advantageous mutations, and specifically to cancer, remains unknown.

A rapidly adapting population faces a double bind: it must quickly acquire often exceedingly rare, adaptive mutations, yet also avoid mutational meltdown. As a result, adaptive processes frequently fail. Indeed, less than 0.1% of species on Earth have adapted fast enough to avoid extinction (20), and similarly, only ∼0.1% of precancerous lesions ever advance to cancer (21). Evolutionary properties of extinction may be exploitable in evolving tumors (22).

Here we investigate how asexual populations such as cancer rapidly evolve new traits while avoiding mutational meltdown. We observed a tug-of-war between beneficial drivers and deleterious passengers that creates two major regimes of population dynamics: an adaptive regime, where the probability of adaptation (cancer) is high, and a nonadaptive regime, where adaptation (cancer) is exceedingly rare. These regimes are separated by an effective barrier, which makes cancer progression an unlikely event. Our model is consistent with cancer genomic and age–incidence data,

Significance

During rapid adaptation, populations start in hostile conditions and must evolve new traits to survive. Development of cancer from a population of precancerous cells within a body is an example of such rapid adaptation. New traits required for cancer progression are acquired by driver mutations in a few key genes. Most mutations, however, are unimportant for progression and can be damaging to cancer cells, termed "passengers." The role these damaging passengers play in cancer and other adaptive processes is unknown. Here we show that driver mutations engage in a tug-of-war with damaging passengers. This tug-of-war explains many phenomena in oncology, suggesting how to develop new therapies and target existing therapies to exploit damaging passengers.

Author contributions: C.D.M., L.A.M., and K.S.K. designed research, performed research, analyzed data, and wrote the paper.

The authors declare no conflict of interest.

*This Direct Submission article had a prearranged editor.

[1]To whom correspondence may be addressed. Email: leonid@mit.edu or korolev@bu.edu.

This article contains supporting information online at www.pnas.org/lookup/suppl/doi:10.1073/pnas.1404341111/-/DCSupplemental.

offers a new interpretation of cancer treatment strategies, and explains a previously paradoxical relationship between cancer mutation rates and clinical outcomes. Most importantly, it suggests that deleterious passengers offer a new, unexploited avenue of cancer therapy.

Results

Model. In simulations, each cell can divide, mutate (in a general sense, i.e., including copy number alterations, chromosomal gains and losses, epigenetic changes, etc.), and die stochastically. Mutations occur during cell divisions with a per-locus rate μ. The frequency of driver mutations per cell division is the overall mutation rate times the number of driver loci in the genome (i.e., target size) T_d; hence, $\mu_d = \mu T_d$. The frequency of passenger mutations is $\mu_p = \mu T_p$. Because there are many more passenger loci than driver loci, $T_p \gg T_d$ (*SI Appendix*).

A single cell's fitness w is determined by its number of accumulated drivers n_d that each increase its fitness by s_d, and its number of accumulated passengers n_p that each decrease fitness by s_p: $w = (1+s_d)^{n_d}(1+s_p)^{-n_p}$. This form assumes that mutations act independently, i.e., no epistasis. In *SI Appendix* and *Discussion*, we consider a simple two-hit form of epistasis. Constant values of s_d and s_p are used here because previous work showed that sampling s from various distributions exhibits qualitatively similar dynamics (12). We assume here and estimate from data below that $s_d > s_p$.

Cell fitness w and the population size N determine the birth and the death rate of that cell. The death rate increases with N according to a Gompertzian function often used to describe cancer dynamics (9). Stochastic cell division (with mutations) and death were modeled using a Gillespie algorithm. To develop the most tractable and foundational model, we assume that all parameters stay constant in time.

Adaptive processes occur within a broad range of evolutionary parameters. For example, μ varies dramatically across cancers (8), whereas estimates of s_d range from 0.0001 (4) to 0.58 (23). Hence, we varied each parameter by 1,000-fold (*SI Appendix*, Table S1) and found that dynamics varied considerably over this range but fell into two broad categories: adaptation (cancer) and extinction (no progression). Previous studies have concluded that passengers minimally affect progression when lethal (7) or if only deleterious in a few housekeeping genes (24); however, we previously presented genomic evidence that cancers accumulate myriad mildly deleterious passengers (12).

A Critical Population Size. Fig. 1*A* shows the dynamics $N(t)$ of individual populations starting at different initial sizes N^0, which correspond to different potential hyperplasia sizes (trajectories begin immediately after a stem cell acquires its first driver; see *SI Appendix* for a discussion of dynamics before this point). Populations exhibit two ultimate outcomes, growth to a macroscopic size (i.e., cancer progression) or extinction, which depend on a critical population size N^*. Larger populations ($N > N^*$) generally commit to rapid growth, whereas smaller populations ($N < N^*$) generally commit to extinction.

To understand the origin of this critical population size N^*, we examined the short-term dynamics of populations. All trajectories follow a reversed sawtoothed pattern (Fig. 1*B*), resulting from a tug-of-war between drivers and passengers (12). When a new driver arises and fixates in the population, the population size

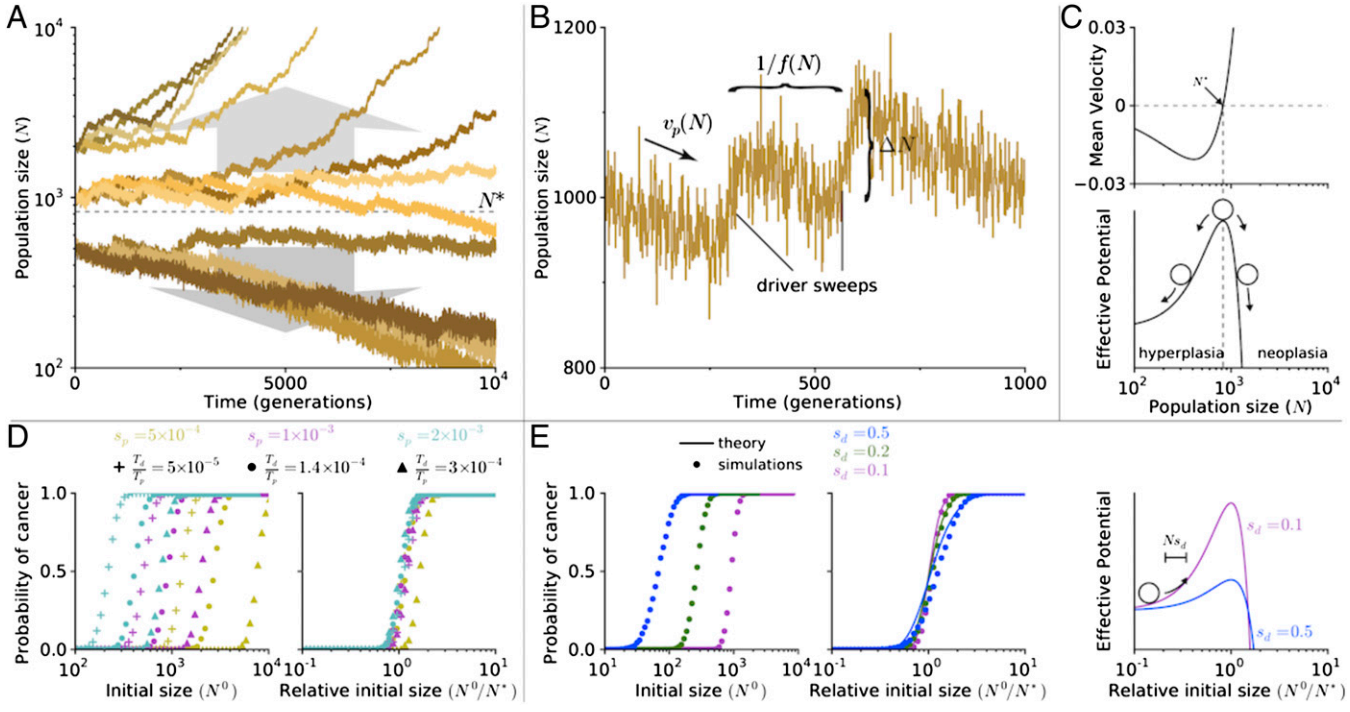

Fig. 1. Tug-of-war between drivers and passengers leads to a critical population size. (*A*) Population size verses time of simulations initiated at various sizes (N^0 = 500, 1,000, or 2,000). For all simulations presented in this paper, $\mu = 10^{-8}$, T_d = 1,400, $T_p = 10^7$, $s_d = 0.1$, and $s_p = 0.001$ (*SI Appendix*, Table S1), unless specified otherwise. (*B*) A segment of a trajectory shows periods of rapid growth and gradual decline. New drivers arrive with a frequency $f(N)$, abruptly increasing the population size by an amount ΔN. Passenger accumulation causes a gradual decline with rate v_p. (*C*) Analytically computed mean velocity of population growth (*Upper*) and an effective barrier (*Lower*) as a function of population size N. Velocity is negative below N^* and positive above it. (*D*) The probability of adaptation (cancer) as a function of initial population size N (*Left*) and a relative initial population size (N/N^*; *Right*) for nine sets of evolutionary parameters. Curves collapse and behave similarly when plotted relative to N^*. (*E*) Same as in *D* for simulations and theory but for different values of s_d. Higher values of s_d leads to a more gradual transition from nonadaptive to adaptive regime. In our formalism, an increase in s_d results in a larger jump size ΔN and lower potential barrier, allowing more populations to overcome the barrier (*Right*).

increases to a new stationary value. In between these rare driver events, the population size gradually declines due to passenger accumulation. The relative rates of these competing processes determine whether a population grows rapidly or goes extinct.

The value of N^* can be identified by considering the average change in population size over time ($\langle dN/dt \rangle$), which is the average population growth due to accumulating drivers (v_d) minus the population decline due to accumulating passengers (v_p). When a new driver fixates, the population size immediately increases by $\Delta N = Ns_d$. These jumps occur randomly at a nearly constant rate $f = \mu_d N s_d$ [a product of the driver occurrence rate $\mu_d N$ and its probability of fixation $s_d/(1 + s_d) \approx s_d$]. Thus, the velocity due to drivers is $v_d = f\Delta N = \mu_d N^2 s_d^2$. Similarly, passengers' velocity $v_p = \mu_p N s_p$ is a product of their rate of occurrence $\mu_p N$, effect on population size Ns_p, and fixation probability (near-neutral $\sim 1/N$; see *SI Appendix* for a more precise estimate). Thus, we obtain

$$\left\langle \frac{dN}{dt} \right\rangle = \mu_p s_p N \left(\frac{N}{N^*} - 1 \right), \qquad [1]$$

where $N^* = \frac{T_p s_p}{T_d s_d^2}$ is the critical population size. In this equation, a population's mean velocity is negative below N^* and positive above N^*, explaining why populations above N^* grow rapidly and populations below N^* continually decline.

These dynamics suggests that N^* constitutes an effective barrier to cancer, which can prevent most cancers from progressing (Fig. 1*C*). Simulations support this conclusion because they exhibit a sharp transition in the probability of progression at N^* (Fig. 1*D*). Indeed, drastically different probability curves collapse onto a single curve when N^0 is rescaled by N^*.

By considering only the average dynamics, we miss the variability of outcomes in adapting populations. In *SI Appendix*, we formulate and solve a stochastic generalization of Eq. **1** that explains the variability of outcomes well (Fig. 1*E*). Outcome variability depends only upon N^* and the strength of drivers s_d. Higher values of s_d lead to larger stochastic jumps ΔN, which increases variability and leads to more gradual changes in the probability of cancer across N^0.

The effects of N^* and s_d on cancer progression can be intuitively understood using a simple random-walk analogy. The population's reverse sawtoothed path abides by a one-dimensional random walk in an effective potential $U_{\text{eff}} = -\int (dN/dt) dN$ (Fig. 1*C*). Akin to chemical reactions activated by thermal energy, cancer progression is a rare event that transitions through an unstable state, requiring a quick succession of driver fixations.

Our analytical formalism indicates that population dynamics depend entirely on two dimensionless parameters: a deterministic mean velocity dependent only upon N/N^* and a stochastic step size of $\sim s_d$. By reducing the complexity of our evolutionary system to two parameters, we were next able to infer their values from real cancers without overfitting.

Model Validation Using Cancer Incidence and Genomics Data. Our model of cancer progression predicts several properties of cancer: the presence of an effective barrier that small lesions seldom overcome, a broad distribution in the number of accumulated drivers and passengers in tumors, and a tug-of-war between drivers and passengers in individual cancers. We looked for evidence of these phenomena in age–incidence data (25) and recent cancer genomics data, which also allowed us to estimate s_d, s_p, and the probability of cancer progression.

Fig. 2*A* presents the incidence rate of breast cancer versus age (25) alongside the predictions from our model and a classic driver-only model (*SI Appendix*). The incidence rate was calculated by assuming that precancerous lesions arise with a constant rate r beginning at birth. Lesions then progress to cancer in time τ with probability $P(\tau)$, determined from simulations (*SI Appendix*, Fig. S1). The age–incidence rate $I(t)$ is then the convolution of $P(\tau)$ with the lesion initiation rate r. Because many lesions never progress and go extinct in our model, the incidence rate saturates at old age: $I_{\max} = r\int_0^\infty P(\tau)d\tau = rP_\infty$, where P_∞ is the probability that a lesion ever progresses to cancer.

Observed age–incidence rates saturate with age, allowing us to estimate the efficiency of cancer progression. We estimate the rate of lesion formation in breast cancer $r \geq 10$ per year, deducible in two ways: by multiplying the number of human breast epithelial stem cells by their rate of mutation into a lesion (*SI Appendix*) or by considering the number of lesions observed in normal breasts (21). By comparing this limit ($r \sim 10\,\text{y}^{-1}$) to the maximum observed breast cancer incidence rate $I_{\max} \sim 10^{-2}$ cancers·year^{-1}, we find that $P_\infty \sim 10^{-3}$, or only $\sim$0.1% of lesions ever progress. Likewise, most other cancer subtypes (84%) plateau at old age, indicating that inefficient progression is common (*SI Appendix*, Fig. S1). These findings are consistent with medical

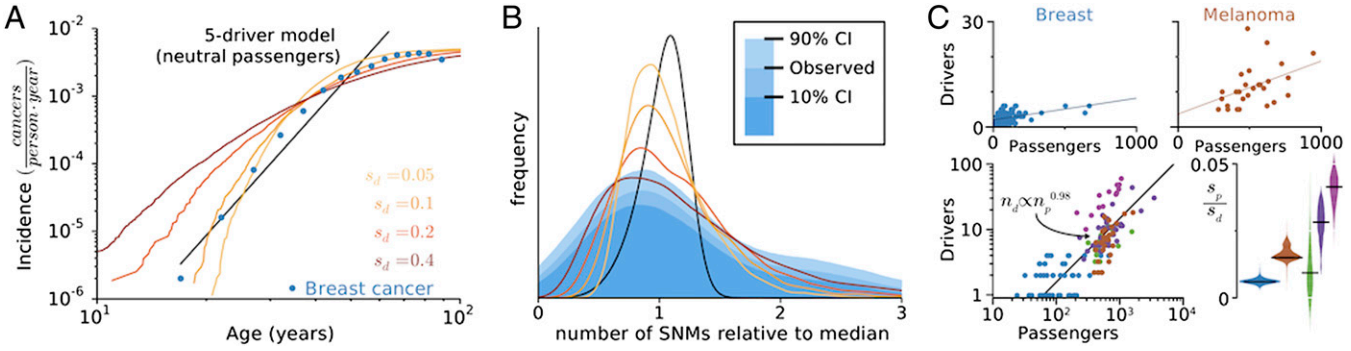

Fig. 2. Signatures of balance between drivers and passengers in incidence and genomics data. (*A*) Predicted and observed breast cancer incidence rates verses age. Incidence rates in our model and the data both plateau at old age, but a traditional driver-only model ($I \propto t^k$) does not. (*B*) Histogram (blue) of the collective number of protein-coding mutations (SNMs) in breast cancer, alongside predicted distributions (lines colors as in *A*). Our model captures the width and asymmetry of the distribution when $s_d = 0.4$, whereas a driver-only model predicts a narrower, less-skewed distribution. (*C*) (*Upper*) The total number of aggregate SCNA and SNM drivers verses the total number of passengers in sequenced tumors (points) fitted by linear regression. (*Lower Left*) Aggregated cancer genomics data plotted on log axes, with the *y* intercept from each subtype's linear fit subtracted [lung cancer (green), colorectal cancer (MIN$^-$, dark purple; MIN$^+$, light purple)]. (*Lower Right*) The distribution of slope values obtained by bootstrapping 10,000 samples of each tumor type. All cancers exhibit positive slopes ($P < 0.08 - 10^{-5}$), suggesting estimates of s_p/s_d of breast, 0.0060 ± 0.0010; melanoma, 0.016 ± 0.003; lung, 0.0094 ± 0.0093; colorectal, MIN$^-$ 0.028 ± 0.007 and MIN$^+$ 0.041 ± 0.006.

observations that very few lesions ever progress to cancer (26, 27). Like our model, these studies also find that most lesions regress to undetectable size. Conversely, in a driver-only model (*SI Appendix*), every lesion eventually progresses to cancer after sufficient time (i.e., $P_\infty = 1$), and incidence rates plateau only if the lesion formation rate is unrealistically low (0.01 per year). Good agreement between age–incidence data and our model is obtained for $s_d \approx 0.1$–0.2.

Recent cancer genomics data offer a new opportunity to validate our model. Specifically, we looked at somatic nonsynonymous mutations (SNMs) and somatic copy-number alterations (SCNAs) from over 700 individual cancer–normal sample pairs (*SI Appendix*, Table S2). Analyzing SNMs and SCNAs separately and in aggregation yielded similar results (*SI Appendix*, Fig. S2 and Table S3). Fig. 2*B* shows a wide and asymmetric distribution of the total number of SNMs in breast cancer. Our model predicts a similarly wide distribution of total SNMs due to the stochastic period that cancers linger at the critical population size N^* while accumulating mutations. To compare these data with various models we normalized the total number of mutations by their median (27) because several evolutionary parameters and sequencing decisions can alter these distributions by a multiplicative factor (*SI Appendix*). Our model agrees with the data when the effect size of drivers is large ($s_d \approx 0.4$). In contrast, a traditional five-driver model (*SI Appendix*) which neglects deleterious passengers and, thus, a critical barrier yields a narrower, less-skewed distribution than observed.

Overall, our model agrees with the 11 most sequenced cancer subtypes best when $s_d \approx 0.1$–0.6 (*SI Appendix*, Fig. S3 and Table S4). These estimates agree with $s_d = 0.16$–0.58 experimentally measured as growth rate changes of mouse cells upon mutations in *p53*, *APC*, or *Kras* (23). These experimental measurements and our estimates are also considerably larger than previous theoretical estimates of $s_d = 0.004$ (4), where cancer progression was modeled as an exponential growth unaffected by passengers. Such a driver-only model fits SNM distributions poorly, and fits suggest that just one to two drivers are needed for cancer (*SI Appendix*, Table S4), which is inconsistent with known biology. Taken together, cancer genomics data and recent experiments (23) strongly support our model and refute the driver-only model.

We then compared the number of drivers and the number of passengers observed in individual cancer samples to our model. Lesions that linger around N^* in our model acquire additional passengers and additional counterbalancing drivers, whereas lesions that progress quickly acquire fewer of each. This predicts a linear relationship: $n_d = s_p/s_d \cdot n_p$ + constant (*SI Appendix*), where the slope provides an estimate of s_p/s_d. We indeed observed a positive linear relationship between n_d and n_p in all tumors studied (Fig. 2*C* and *SI Appendix*, Table S3; $P < 0.08$–10^{-6}). Linearity was confirmed by regressing the aggregated data in log–log axes (Fig. 2*C*), which yielded $n_d \sim n_p^{0.98}$, consistent with $n_d \sim n_p$. Regressing n_d on n_p and using 10^4 bootstrapped samples to estimate the confidence, we obtain an $s_p/s_d \sim 0.005$–0.05 (Fig. 2*C*). Using our estimate $s_d \approx 0.1$–0.6, we obtain a damaging effect of a passenger mutation $s_p \approx 5 \cdot (10^{-4}$–$10^{-2})$. These estimates are consistent with effects of germ-line SNMs in humans where 64% of mutations decrease fitness by 10^{-5}–10^{-2} (28). In summary, this analysis shows that passengers are indeed deleterious and ~100× weaker than drivers.

We considered and refuted several alternative explanations for the observed positive linear relationship between drivers and passengers. First, variation in the tumor stage or the rate/mechanism of mutagenesis cannot explain the observed relationship (*SI Appendix*, Table S3). Second, SCNAs and SNMs are uncorrelated, so the linear relationship could not result from their differing effect sizes (*SI Appendix*, Fig. S2 and Table S3). Because the data disagree with these alternate hypotheses, we conclude that cancer indeed proceeds as a tug-of-war between drivers and passengers.

A Critical Mutation Rate. By simulating cancer progression over a broad range of evolutionary parameters (*SI Appendix*, Fig. S4), we observed another barrier to cancer: a critical mutation rate, above which the probability of cancer is exceedingly low (Fig. 3*A*). Through further analytical treatment (*SI Appendix*), we found that this mutational barrier is created and determined by the load of segregating (unfixed) passengers in the population. The origin of a critical mutation rate can be understood by considering the number of segregating passengers per cell, previously shown to be Poisson distributed with mean μ_p/s_p, during mutation–selection balance (29). The average fitness reduction of a cell due to this mutational load is then μ_p. If this fitness reduction exceeds the benefit of a new driver ($\mu_p > s_d$), then drivers seldom fixate (17, 30) (Fig. 3*C*). Hence, cancer is extremely rare above the critical mutations rate $\mu^* = s_d/T_p$.

Fig. 3*A* shows that this simple argument accurately predicts the location of the critical mutation rate. By incorporating more details about segregating passengers and selection against them (*SI Appendix*), we explain observed simulation dynamics well across the entire phase space (Fig. 3 *A* and *B* and *SI Appendix*, Fig. S4).

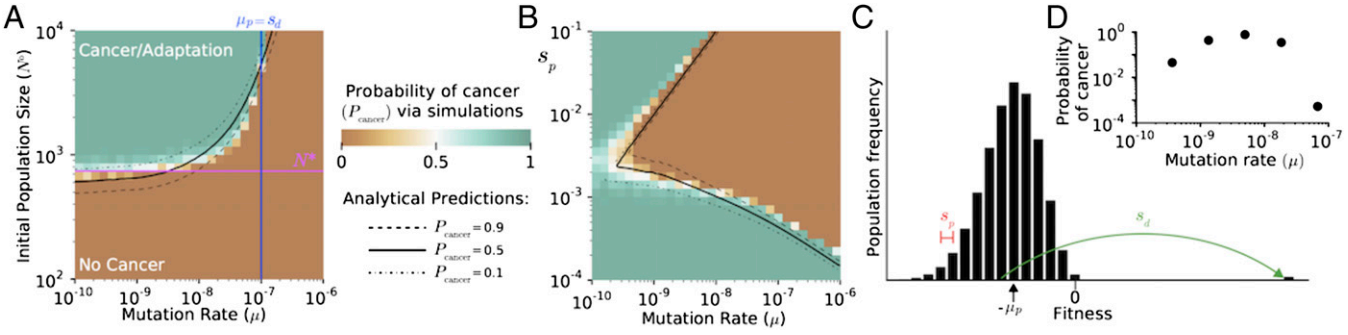

Fig. 3. Effect of mutation rate on cancer dynamics. (*A*) The probability of cancer (adaptation) computed by simulations across mutation rates and initial population sizes. Evolutionary parameters partition adaptation into a regime where cancer is almost certain (green) and a regime where it is exceedingly rare (brown), accurately predicted by theoretical estimates of N^* (magenta) and μ^* (blue). A theory incorporating passenger interference with driver sweeps and selection against passengers explains simulations well (black lines). (*B*) Cancer probability as a function of μ and s_p ($N^0 = 10^3$). Theory (black lines) accurately reproduces the complex transition between regimes. (*C*) Diagram illustrating how the load of segregating (unfixed) passengers influences relative cell fitness and the probability of a driver fixating. Hitchhiking passengers reduce a driver's fitness benefit and probability of fixation. (*D*) Probability of cancer constrained to grow within a human lifespan ~60 years, 10^4 generations, with $N^0 = 10^3$ for various mutation rates exhibits an optimum mutation rate.

This analysis offers a new mode by which mutational meltdown operates. Whereas prior models of mutational meltdown consider deleterious mutations in isolation (16), we find that mutational meltdown can occur when deleterious mutations inhibit the accumulation of advantageous mutations.

When cancer progression is constrained to develop within a human lifetime, we observe an optimum mutation rate for the probability of cancer ($\mu^{opt} = 10^{-9}$–10^{-8} nucleotide^{-1}·generation^{-1}; Fig. 3*D*), similar to experimentally measured rates in cancer of 10^{-8} (7). Above μ^{opt}, population meltdown is very common, whereas below μ^{opt}, progression is too slow.

The Adaptive Barrier and Critical Mutation Rate Explain Cancer Treatment Outcomes. Chemotherapy and radiation are valued for their ability to kill rapidly dividing cells; however, our model shows that the elevation of mutation rates (including SCNAs and aneuploidy) by these therapies dramatically affects cancer survival. We use the phase diagrams from Fig. 3 to rationalize outcomes of these and other treatments.

In Fig. 4*A*, we present evolutionary paths of cancers—from hyperplasia, to cancer, to treatment, and to relapse or remission—on top of the phase diagrams described above. Treatments succeed if they push cancer into the nonadaptive regime (where the probability of growth is low) and fail if they do not. Our model suggests that chemotherapy succeeds, in part, because it moves cancers across the mutational threshold μ^*. Above this threshold, drivers seldom overpower the load of segregating passengers, making readaptation difficult. Driver-targeted therapies (that eliminate an oncogene's benefit) must bring $n < N^*$ to succeed.

Cancers with higher loads of mutations/alterations are closer to the critical mutation rate and should be most susceptible to mutagenic meltdown. Several recent studies (31–33) found that patient survival from breast (all subtypes) and ovarian cancer was greatest when tumors harbored exceptionally high levels of chromosomal alterations. These findings are paradoxical for all previous models of cancer (31), where a greater mutation rate always accelerates cancer, yet fully consistent with our model (Fig. 4*B*).

Treatments exploiting cancer's load of deleterious passengers remain unexplored. Fig. 4*C* shows that a relatively mild threefold to fivefold increase of the deleterious effect of passengers s_p causes complete remission. Increasing s_p is doubly effective because it exacerbates accumulated passengers and slows down future adaptation. Below we discuss possible treatment strategies that would increase s_p.

Increases in μ work synergistically with increases in s_p in our model (*SI Appendix*, Fig. S6). Hence, combinations of mutagenic chemotherapy with treatments elevating the cost of passengers may be most effective; these therapies should further synergize with driver-targeted therapies.

Discussion

We present an evolutionary model of rapid adaptation incorporating rare, strongly advantageous driver mutations and frequent, mildly deleterious passenger mutations. In this tug-of-war process, populations either succeed and adapt or fail and go extinct. Simulations and theory identify two regimes of dynamics: one where populations almost always adapt and another where they almost always fail. The complex stochastic dynamics of this process is accurately described as simple diffusion over a potential barrier located at a critical population size separating the two regimes. This general framework for adaptive asexual populations effectively characterizes the dynamics of cancer progression and therapeutic responses.

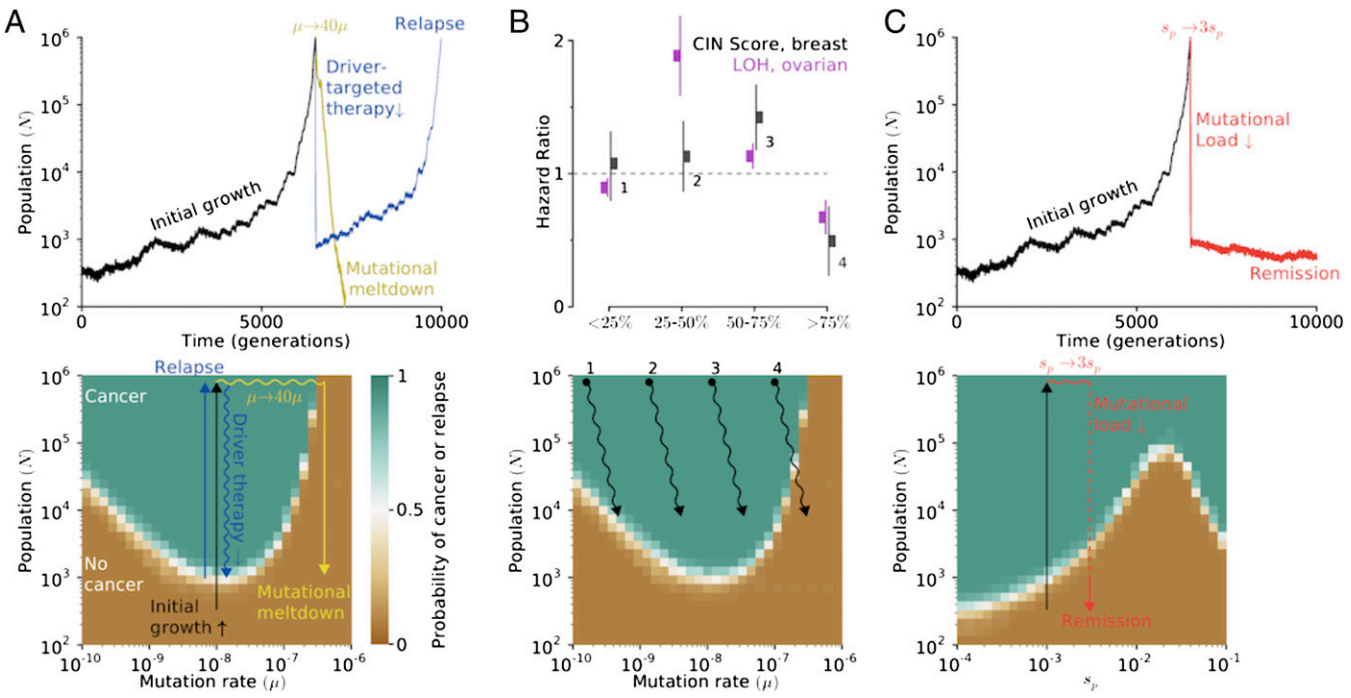

Fig. 4. Mapping and interpreting treatment outcomes. (*A*, *Upper*) An adapted population (cancer) can be reverted to extinction by increasing the mutation rate (mutagenic chemotherapy) or by decreasing the population size (e.g., surgery or cytotoxic chemotherapy). (*Lower*) Our phase diagrams explain therapeutic outcomes: therapies that alter evolutionary parameters enough to push it outside of the adaptive regime cause continued population collapse; those that do not readapt and relapse. (*B*, *Upper*) Cancers with intermediate mutational loads are the most aggressive (31, 33), whereas patients with very high level of chromosomal instability are most effectively treated. (*Lower*) This result is well explained by our phase diagrams, where cancers with high mutation rates are susceptible to mutational meltdown, yet paradoxical for all previous evolutionary models of cancer. We believe traditional therapies decrease population size and may increase the mutation rate. (*C*) Threefold increase in the effect of passenger mutations leads to rapid population meltdown below N^*, without relapse.

We show that the late onset of cancer, evident in age–incidence curves, can be explained by a passenger-generated barrier to cancer and does not require more complex models of cancer progression (e.g., a specific order of mutations, or multihit model, or variable mutation rate). We also considered a commonly used two-hit model in *SI Appendix*, where the first driver confers no fitness benefit, whereas two drivers confer a strong cumulative effect. This two-hit model also exhibits a barrier to cancer and behaves similarly to our model (*SI Appendix*, Fig. S7), yet with an effectively larger N^* and s_d.

Our framework suggests that most normal tissues reside in a regime where cancer progression is exceedingly rare. Most lesions fail to overcome the adaptive barrier at N^*. This implies that observed tumors acquired drivers faster than a mean trajectory and may be testable via phylogenetic analysis.

Clinical cancers, on the contrary, reside above the adaptive barrier in a rapidly adapting state. Successful therapies must push a cancer below this adaptive barrier N^* or increase the mutation rate above the critical value μ^*.

We tested our model and estimated its parameters using age–incidence curves, cancer exome sequences from ∼1,000 tumors in four cancer subtypes, and data on clinical outcomes. Age–incidence curves support our hypothesis that nearly all lesions fail to progress and allowed us to estimate the fitness benefit of a driver as $s_d \approx 0.1–0.6$, in good agreement with direct experimental measurements (23). Genomics data also affirmed that a damaging effect of a nonsynonymous passenger is 100 times smaller than the effect of a driver, but passengers are 100 times more numerous than drivers. Taken together, these data support the notion of a tug-of-war between rare large-effect drivers verses frequent mildly deleterious passengers.

Clinicians could exploit deleterious passengers by either increasing the mutation/alteration rate in cancers with already high mutation rates or by increasing the deleterious effect of passengers. Clinical data indeed show that cancers with a higher load of chromosomal alterations, closer to μ^*, respond better to treatments (31–33). PARP inhibitors, which increase DNA damage in *BRCA1/2*-positive tumors, may already be curing patients by inducing mutational meltdown (34).

Passenger mutations and alterations can be deleterious by gain-of-function toxicity via proteotoxic/misfolding stress (14, 35) or by eliciting an immune response to mutated epitopes (15). Their damage to cancer cells could be magnified by (*i*) inhibiting unfolded protein response (UPR) pathways and proteasomes (14), (*ii*) hyperthermia that further destabilizes mutated proteins and clogs UPR pathways (36), or (*iii*) activating an immune response (37). All these strategies are in clinical trials, yet none are believed to work by exacerbating passengers' deleterious effects. Our alternative explanation for their efficacy suggests that these therapies will be most effective in combination and in cancers with many passengers.

This study focused on the evolution of cancer, but our model should generalize to other adaptive asexual processes. Consider a small population entering a new environment. Fluctuations in its size often lead to its extinction. Occasionally, however, the population may acquire several new highly advantageous traits for this new environment, allowing it to rapidly expand its size and avert extinction. Both its evolutionary parameters (18) and behavior (38) mirror our model. Our mathematical framework further explains why these populations sometimes adapt, yet often fail.

Materials and Methods

Simulations used a first-order Gillespie algorithm (12). Drivers and passengers were classified in the studies where they were first identified. See *SI Appendix* for details.

ACKNOWLEDGMENTS. We are grateful to Shamil Sunyaev, Gregory Krykov, Geoffrey Fudenberg, Maxim Imakaev, and Anton Goloborodko for many productive discussions. C.D.M. and L.A.M. were supported by National Cancer Institute Grant U54CA143874. K.S.K. was supported by the Pappalardo Fellowship in Physics at Massachusetts Institute of Technology.

1. Kawashima Y, et al. (2009) Adaptation of HIV-1 to human leukocyte antigen class I. *Nature* 458(7238):641–645.
2. Zhang Q, et al. (2011) Acceleration of emergence of bacterial antibiotic resistance in connected microenvironments. *Science* 333(6050):1764–1767.
3. Wright SI, et al. (2005) The effects of artificial selection on the maize genome. *Science* 308(5726):1310–1314.
4. Bozic I, et al. (2010) Accumulation of driver and passenger mutations during tumor progression. *Proc Natl Acad Sci USA* 107(43):18545–18550.
5. Cameron TC, O'Sullivan D, Reynolds A, Piertney SB, Benton TG (2013) Eco-evolutionary dynamics in response to selection on life-history. *Ecol Lett* 16(6):754–763.
6. Hanahan D, Weinberg RA (2011) Hallmarks of cancer: The next generation. *Cell* 144(5):646–674.
7. Beckman RA, Loeb LA (2005) Negative clonal selection in tumor evolution. *Genetics* 171(4):2123–2131.
8. Lawrence MS, et al. (2013) Mutational heterogeneity in cancer and the search for new cancer-associated genes. *Nature* 499(7457):214–218.
9. Domingues JS (2012) Gompertz model: Resolution and analysis for tumors. *J Math Model Appl* 1(7):70–77.
10. Lawrence MS, et al. (2014) Discovery and saturation analysis of cancer genes across 21 tumour types. *Nature* 505(7484):495–501.
11. Zack TI, et al. (2013) Pan-cancer patterns of somatic copy number alteration. *Nat Genet* 45(10):1134–1140.
12. McFarland CD, Korolev KS, Kryukov GV, Sunyaev SR, Mirny LA (2013) Impact of deleterious passenger mutations on cancer progression. *Proc Natl Acad Sci USA* 110(8):2910–2915.
13. MacArthur DG, et al.; 1000 Genomes Project Consortium (2012) A systematic survey of loss-of-function variants in human protein-coding genes. *Science* 335(6070):823–828.
14. Sheltzer JM, Amon A (2011) The aneuploidy paradox: Costs and benefits of an incorrect karyotype. *Trends Genet* 27(11):446–453.
15. Vesely MD, Schreiber RD (2013) Cancer immunoediting: Antigens, mechanisms, and implications to cancer immunotherapy. *Ann N Y Acad Sci* 1284:1–5.
16. Lynch M (2008) The cellular, developmental and population-genetic determinants of mutation-rate evolution. *Genetics* 180(2):933–943.
17. Johnson T, Barton NH (2002) The effect of deleterious alleles on adaptation in asexual populations. *Genetics* 162(1):395–411.
18. Goyal S, et al. (2012) Dynamic mutation-selection balance as an evolutionary attractor. *Genetics* 191(4):1309–1319.
19. Neher RA, Shraiman BI (2012) Fluctuations of fitness distributions and the rate of Muller's ratchet. *Genetics* 191(4):1283–1293.
20. May R, Lawton J, Stork N (1995) *Assessing Extinction Rates* (Oxford Univ Press, Oxford).
21. Page DL, Dupont WD, Rogers LW, Rados MS (1985) Atypical hyperplastic lesions of the female breast. A long-term follow-up study. *Cancer* 55(11):2698–2708.
22. Korolev KS, Xavier JB, Gore J (2014) Turning ecology and evolution against cancer. *Nat Rev Cancer* 14(5):371–380.
23. Vermeulen L, et al. (2013) Defining stem cell dynamics in models of intestinal tumor initiation. *Science* 342(6161):995–998.
24. S Datta R, Gutteridge A, Swanton C, Maley CC, Graham TA (2013) Modelling the evolution of genetic instability during tumour progression. *Evol Appl* 6(1):20–33.
25. National Cancer Institute (2014) *Surveillance, Epidemiology, and End Results (SEER) Program Research Data (1973–2011).* Available at http://seer.cancer.gov/archive/csr/1975_2009_pops09/results_single/sect_01_table.10_2pgs.pdf. Accessed March 7, 2014.
26. Bota S, et al. (2001) Follow-up of bronchial precancerous lesions and carcinoma in situ using fluorescence endoscopy. *Am J Respir Crit Care Med* 164(9):1688–1693.
27. Tong WWY, et al. (2013) Progression to and spontaneous regression of high-grade anal squamous intraepithelial lesions in HIV-infected and uninfected men. *AIDS* 27(14):2233–2243.
28. Boyko AR, et al. (2008) Assessing the evolutionary impact of amino acid mutations in the human genome. *PLoS Genet* 4(5):e1000083.
29. Haigh J (1978) The accumulation of deleterious genes in a population—Muller's Ratchet. *Theor Popul Biol* 14(2):251–267.
30. Peck JR (1994) A ruby in the rubbish: Beneficial mutations, deleterious mutations and the evolution of sex. *Genetics* 137(2):597–606.
31. Birkbak NJ, et al. (2011) Paradoxical relationship between chromosomal instability and survival outcome in cancer. *Cancer Res* 71(10):3447–3452.
32. Ciriello G, et al. (2013) Emerging landscape of oncogenic signatures across human cancers. *Nat Genet* 45(10):1127–1133.
33. Wang ZC, et al.; Australian Ovarian Cancer Study Group (2012) Profiles of genomic instability in high-grade serous ovarian cancer predict treatment outcome. *Clin Cancer Res* 18(20):5806–5815.
34. Lee AJX, Swanton C (2012) Tumour heterogeneity and drug resistance: Personalising cancer medicine through functional genomics. *Biochem Pharmacol* 83(8):1013–1020.
35. Jordan DM, Ramensky VE, Sunyaev SR (2010) Human allelic variation: Perspective from protein function, structure, and evolution. *Curr Opin Struct Biol* 20(3):342–350.
36. Rossi-Fanelli A, Cavaliere R, Mondov B, Moricca G (1977) *Selective Heat Sensitivity of Cancer Cells* (Springer, Berlin), pp 1–192.
37. Segal NH, et al. (2008) Epitope landscape in breast and colorectal cancer. *Cancer Res* 68(3):889–892.
38. Bell G, Gonzalez A (2009) Evolutionary rescue can prevent extinction following environmental change. *Ecol Lett* 12(9):942–948.